AAPS PharmSciTech 2002; 3 (4) article 34 (http://www.aapspharmscitech.org).

Effects of Physical Properties for Starch Acetate Powders on Tableting

Submitted: August 15, 2002; Accepted: December 9, 2002

Ossi Korhonen[1], Seppo Pohja[1], Soili Peltonen[2], Eero Suihko[1], Mika Vidgren[1], Petteri Paronen[1], Jarkko Ketolainen[1]

[1]Department of Pharmaceutics, University of Kuopio, PO Box 1627, FIN-70211 Kuopio, Finland

[2]VTT Chemical Technology, Materials Technology, PO Box 21, FIN-05210 Rajamäki, Finland

ABSTRACT

The aim of the study was to investigate particle and powder properties of various starch acetate powders, to study the effect of these properties on direct compression characteristics, and to evaluate the modification opportunity of physical properties for starch acetate powders by using various drying methods. At the end of the production phase of starch acetate, the slurry of starch acetate was dried using various techniques. Particle, powder, and tableting properties of end products were investigated. Particle size, circularity, surface texture, water content and specific surface area varied according to the particular drying method of choice. However, all powders were freely flowing. Bulk and tapped densities of powders varied in the range of 0.29 to 0.44 g/cm^3 and 0.39 to 0.56 g/cm^3, respectively. Compaction characteristics revealed that all powders were easily deformed under compression, having yield pressure values of less than 66 MPa according to Heckel analysis. All powders possessed a significant interparticulate bond-forming capacity during compaction. The tensile strength values of tablets varied between 10 and 18 MPa. In conclusion, physical properties of starch acetate could be affected by various drying techniques. A large specific surface area and water content above 4% were favorable properties by direct compression, especially for small, irregular, and rough particles.

KEYWORDS: starch acetate, drying techniques, powder, tablet, excipient.

Corresponding Author: Ossi Korhonen, Department of Pharmaceutics, University of Kuopio, PO Box 1627, FIN-70211 Kuopio, Finland.Telephone: +358 17 162496; Facsimile: +358 17 162252; E-mail: Ossi.Korhonen@uku.fi

INTRODUCTION

Starch acetates are novel multifunctional excipients for direct compression.[1,2] Production of starch acetates consist of 4 main phases: (1) synthesis, (2) precipitation, (3) filtration and washing, and (4) drying of the starch acetate slurry.[3] During synthesis, starch is allowed to react with acetic acid anhydride, with sodium hydroxide as a catalyst, in a pressurized and heated reaction vessel. After the reaction phase, the mixture is allowed to cool and starch acetate is precipitated from the water with vigorous mixing. The precipitate is then filtered and washed with water. In the final phase, the wet starch acetate mass is dried.

By varying reaction conditions, starch acetates having degrees of substitution from near 0 to 3.0 can be produced. Most of the physicochemical and mechanical properties of starch acetates strongly depend on the degree of substitution.[1] As the degree of substitution increases from near 0 to 3.0, the nature of the starch acetate changes from hydrophilic to more hydrophobic and, simultaneously, the interparticular bonding capacity increases greatly. In addition, the drug release rate slows as the degree of substitution for starch acetate increases.

It is well recognized that many manufacturing processes, like precipitation or drying, have a significant effect on the physical and solid-state properties of materials and subsequent formulation characteristics.[4,5] In this study, the manufacturing procedure of starch acetate was standardized up to the drying phase. The final drying of the starch acetate was done by using different dryers. The aims of this study were to characterize the particle and powder properties of various starch acetates, to investigate the effects of these properties on the subsequent compaction characteristics, and to evaluate the modification opportunity of starch acetate by using various drying techniques.

Table 1. Dryers and Drying Parameters*

Drying Method	Drying Temp (ºC)	Vacuum (mbar)	Batch Size (kg)	Yield (%)	Drying Time (min)	Residual Moisture (%)	Batch Code
Lödige VT50	70†	100	6.3	66	120	6	Batch 1
Drais turbudry TD20	45-92‡	45-170	70	81	90	1	Batch 2
Anhydro tunnel-shaped fluid-bed dryer	140§	-	nd	nd	240	5	Batch 3
Laboratory spin flash dryer	140§	-	12	89	75	5	Batch 4

*nd indicates not determined.
†Jacket temperature.
‡Material temperature during drying.
§Air inlet temperature (outlet temperature was 70ºC in batch 4, but outlet temperature of batch 3 was not known).

MATERIALS AND METHODS

Materials

Starch acetate was manufactured by VTT as described by Paronen et al[3] (VTT, Chemical Technology, Materials Technology, Finland). The degree of substitution on starch acetate (2.6) was determined by gel permeation chromatography. Microcrystalline cellulose (MCC) (Avicel PH101, FMC) and dicalcium phosphate dihydrate (DCP) (Emcompress, E. Mendell) were chosen as reference materials and used as received. All powdered materials were stored at 33% relative humidity and at room temperature for 7 days prior to any experiments.

Methods

The starch acetate slurry was dried by using 4 different dryers: batch 1 (Lödige VT50, Gerb Lödige Maschinenbau GmgH, Paderporn, Germany); batch 2 (Drais turbudry TD20, Draiswerke GmbH, Speckweg, Germany); batch 3 (Anhydro tunnel-shaped fluid-bed dryer, APV Anhydro AS, Copenhagen, Denmark); and batch 4 (Laboratory Spin Flash dryer, APV Anhydro AS, Copenhagen, Denmark) (**Table 1**, **Figure 1**). Residual water was measured gravimetrically. Dryers of batches 1 and 2 were horizontal vacuum rotary dryers.[6] The most well known horizontal vacuum rotary dryer consists of a stationary-jacketed cylindrical shell with mixing blades inside, in addition to heating and vacuum components. The removal of water from the studied material was achieved by heating, vacuuming, and mixing. The dryer for batch 3 was a fluid bed dryer in which warm gas, usually air, was passed through the powder bed, causing both the evaporation of water and powder mixing.[7] The dryer for batch 4 was a mechanical agitated fluid bed dryer, or spin flash dryer. Basically this dryer was similar to the fluid bed dryer, but contained an additional mechanical agitator.

Particle and powder properties

The particle shape and surface texture were visually evaluated by scanning electron microscope (SEM) (Jeol JSM-35, Tokyo, Japan). The particle size and size distribution of the powder was determined by laser diffractometer (Malvern Instruments Ltd, Mastersizer 2000, Worcestershire, England). Particle in liquid (ethanol) method was used. Particle agglomerates were decomposed using ultrasound. Use of ultrasound was stopped when particle size did not change between individual measurements. Then, particle size was determined as the mean of 10 measurements. Results are expressed as D (ν, 0.1), D (ν, 0.5), and D (ν, 0.9), in which D (ν, 0.1), D (ν, 0.5), and D (ν, 0.9) are sizes (D) in microns at which 10%, 50%, and 90% of the sample is smaller. Term "ν" indicates that particle size determination has based on the volume of sphere that is equal with measured particle. Particle size distribution was determined as a span, which is a measure of width of the size distribution. The narrower the distribution, the smaller the span becomes. The span was calculated as in Equation 1.

$$\text{Span} = [D(v, 0.9) - D(v, 0.1)] / D(v, 0.5) \quad (1)$$

The specific surface area (SSA) of powdered samples was determined by single-point BET method (Micromeritics Flowsorb II 2300, Norgross, GA). A nitrogen/helium (70%/30%) gas mixture was used as a measuring gas. Powders were dried under vacuum and +40ºC for 24 hours before determination. Results are expressed as the mean of 5 determinations.

Water content of the powders was measured by the gravimetric method. Powders were stabilized at 33% relative humidity at room temperature prior to the measurements. Stabilized powder samples were placed in petri dishes and dried in the oven at +170ºC (Termaks, Ber

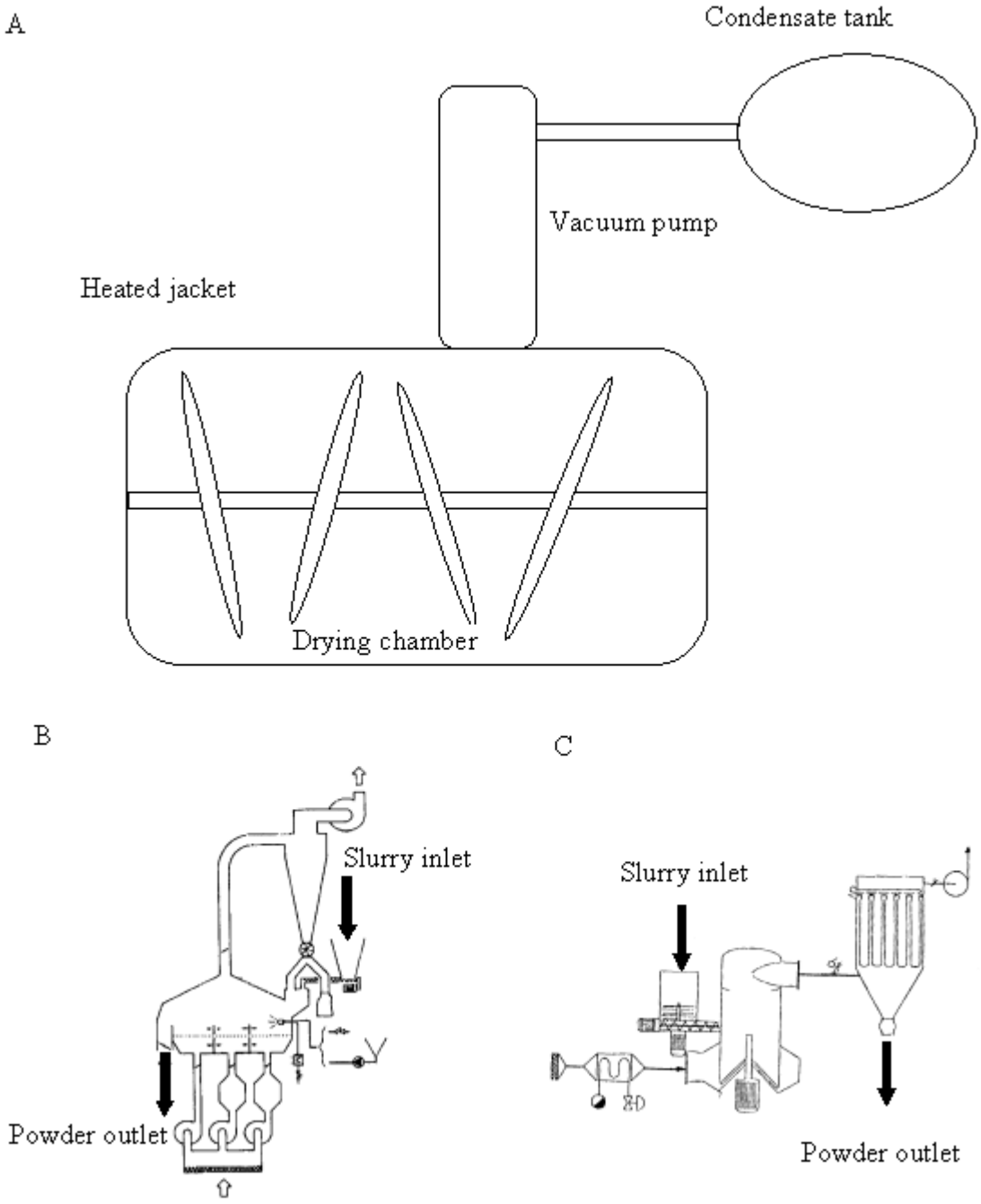

Figure 1. Simplified dryers layout drawing. A = Horizontal vacuum rotary drier; B = Fluid bed drier; and C = Spin flash drier.

gen, Norway). The weight loss was obtained by accurately weighing the sample after 24 hours. Results are expressed as the mean of 3 parallel determinations.

Particle densities (Ph Eur 2.2.24) of the powders were measured with a multipycnometer (Quanta Chrome, Syosset, NY) using helium as a measuring gas. Bulk density was determined by carefully pouring the powder (about 20 g) into a glass cylinder, then calculating the mass of powder by dividing it with the powder volume. For tap density, the cylinder was tapped for 10 minutes (Erweka SVM, Erweka Apparatebau GmbH, Heusenstamm, Germany). The tap density was calculated as the bulk density, as describe above. Densities were determined as the mean of 5 measurements.

The volume reduction of a powder due to tapping was evaluated using the Kawakita equation (Equation 2)[8]:

$$N/C = N/a + 1/ab \qquad (2)$$

where N is the number of taps, and both a and b are constants. The constants of Kawakita equation can be used to estimate the flow and cohesiveness properties of powders. Constant a describes the compressibility and constant $1/b$ describes cohesive properties of powders or the fastness of how the final packing stage is achieved. Term C describes volume reduction during the tapping treatment and was calculated by Equation 3:

$$C = (V_0 - V) / V_0 \quad (3)$$

where V_0 is the loose volume of the powder column before tapping, and V is the volume of the powder column after a certain number of taps (V).

The angle of repose was determined from the dimensions of the powder pile, which formed when 20 g of powder sample was placed in a funnel and allowed to flow. The orifice of the funnel was fixed 6 cm above the base. Results are expressed as the mean of 5 determinations.

Tableting properties

Tablets were compressed with a compaction simulator (PuuMan Ltd, Kuopio, Finland) using a 10-mm diameter flat-faced punch and die set. A compression pressure of 200 MPa was applied at rate of 30 mm/s. The upper punch followed a saw-tooth profile, while the lower punch was kept stationary during compression. The weight of tablets was adjusted to give a theoretical thickness of 1.5 mm at zero porosity, by taking into account the diameter of the die and the particle density of the material. Force-displacement data were collected from 4 parallel compressions and corrected according to punch deformations.

Volume reduction properties of the powders were evaluated from the force-displacement data using the Heckel equation (Equation 4)[9,10]:

$$ln\,(1/1 - D)) = kP + A \quad (4)$$

where D is the relative density of a powder column at the compression pressure P. The reciprocal of slope (k) from the Heckel plot is referred to as the yield pressure (P_y). Constant A in the Heckel equation is related to the die filling and particle rearrangement phases before deformation and particle bonding. *ln* is the natural logarithm. The relative densities of the powder beds at the very beginning of compression were calculated by Equation 5:

$$D_A = D_0 + D_b \quad (5)$$

where D_0 describes the relative density because of die filling, D_b represents the particle rearrangement phase, and D_A includes both the die filling and particle rearrangement phases.

Breaking strength, weight, and dimensions of tablets were measured for 5 tablets 24 hours after tableting. The breaking strength was measured with a universal tester (CT-5 tester, Engineering Systems, Nottingham, England) operated at a constant load cell speed of 1 mm/min. Tensile strength of tablets was calculated according to Fell and Newton.[11] Porosity (ε) of tablets was calculated according to Equation 6:

$$\varepsilon = [1 - (m/V) / \rho_m] \times 100\% \quad (6)$$

where m is the weight of the tablets, V is the volume of the tablets, and ρ_m is the particle density of materials.

The percentage elastic recovery (ER) of tablets was measured using Equation 7:

$$ER = [(H_t - H_m) / H_m)] \times 100\% \quad (7)$$

where H_m is the height of the tablet at the maximum compression pressure and H_t is the tablet height 24 hours after compression.

RESULTS AND DISCUSSION

Particle properties

All dryers removed the bulk water effectively, but produced differing particles. Only 1 drying was performed for each dryer type, therefore estimation of the process reproducibility was not possible. In the case of batch 1, relatively low drying temperature and moderate vacuum induced quite slow removal of water, which resulted in large spherical particles having a smooth surface texture and wide particle size distribution (**Table 2**, **Figures 2** and **3**). An almost total absence of small particles might be due to the vacuum filter, which may have allowed small particles to pass through. Batch 2 was also dried at relatively low temperature, but lower vacuum, and the more powerful agitation together caused a more effective removal of water (residual moisture 1%) than with batch 1. Due to the fast drying and powerful agitation, the particles of batch 2 were smaller, more irregular, and had larger specific surface area than the particles from batch 1 (**Table 2**, **Figure 2**). Particle size distribution was narrower than that of batch 1 (**Table 2**, **Figure 3**). The drying of batches 3 and 4 was based on the fluid-bed method. Vigorous mixing of the fluidized particles and excellent heat transfer properties between the solid and gas phases led to the rapid evaporation of water. This method produced small, irregular, and porous particles having a large specific surface area. Particle size distribution of batches 3 and 4 was narrower than that of batches 1 and 2 (**Table 2**, **Figure 3**). Fluid-bed apparatus have also been used in granulation. Among the particles of batch 3, agglomerates or granules could be observed (**Figure 2**). Ordinarily, granulation goes from the dry powder to the wet state, but in our case the reverse was observed. In the beginning, the powder was in an overwetted state and then dried past the state of granule

Table 2. Material Properties*

Drying Method	Particle Density (g/cm^3)	Particle Size D(v, 0.1) (μm)	Particle Size D(v, 0.5) (μm)	Particle Size D(v, 0.9) (μm)	Particle Size Distribution (Span)	Specific Surface Area (m^2/g)	Water Content (%)
Batch 1	1.36 (0.01)	24 (1)	165 (9)	851 (97)	5.0	4.84 (0.02)	2.0 (0.1)
Batch 2	1.37 (<0.01)	7 (<1)	34 (1)	132 (4)	3.7	6.71 (0.07)	1.3 (0.1)
Batch 3	1.38 (0.01)	16 (<1)	60 (1)	159 (22)	2.4	9.32 (0.33)	1.8 (0.1)
Batch 4	1.37 (0.01)	9 (<1)	45 (1)	164 (22)	3.4	10.46 (0.09)	2.2 (0.1)
MCC	1.66 (<0.01)	20 (<1)	53 (<1)	118 (<1)	1.8	1.01 (0.01)	4.4 (0.2)
DCP	2.33 (<0.01)	88 (1)	172 (1)	288 (2)	1.2	0.67 (<0.01)	0.2 (0.1)

*SD appears in parentheses. MCC indicates microcrystalline cellulose and DCP, dicalcium phosphate dihydrate.

or agglomerate formation. In the particles of batch 4, no granule or agglomerate formation was observed because of the additional agitation of the spin-flash drier, which disrupted possible granules or agglomerates (**Figure 2**). The particle densities of the prepared powders were practically equal, regardless of the different particle properties (**Table 2**). The specific surface areas of the particles correlate with particle size, shape, and surface texture properties (**Table 2**).

Powder properties

One of the most important factors affecting the bulk density of a powder and its flow properties is the interparticulate interaction.[12] Favorable particle properties and the optimal presence of water diminish the cohesiveness of the powder, resulting in an increased bulk density and enhanced flowability. The greatest bulk density was observed in batch 2 (**Table 3**), which had a rather small particle size, moderate specific surface area, and low water content (Table 2). Batch 4, however, had the lowest bulk density due to the small particle size, a large specific surface area, and high water content (**Table 2**).

The tap densities were approximately equal between different batches, excluding batch 2, in which tap density was considerably greater (**Table 3**). The angle of repose values (all under 25°C) indicated that all studied powders were freely flowing (**Table 3**). Some contradiction may arise from the inaccurate determination of powder pile dimensions.

Kawakita constants indicate the behavior of the powder from the bulk density state to the tap density state. The constants of the Kawakita equation were resolved from the slope and intercept of the line from graphs *N/C* versus *C* (**Table 3**). According to published results, small values of constants *a* (compressibility, or the amount of densification due to tapping) and 1/*b* (cohesiveness, or how fast or easily the final packing state was achieved) indicate good flowability and small cohesiveness.[13,14] From our results, it was difficult to make comparable conclusions in this regard. Batch 1 densified the least (small compressibility value) but attained the final packing state most slowly. On the other hand, batch 4 densified considerably but achieved the final packing state rather quickly. Comparisons between starch acetates and MCC illustrated that the powder properties of MCC were poor compared with starch acetates due to its fiber-like particle shape (Figure 2). The huge 1/*b*-value of DCP might arise from the slow fragmentation of DCP and rearrangement of these new fragments during tap treatment.

Packing fractions

Relative densities (D_0, D_b, and D_A) of the powder beds at the beginning of the compression phase are shown in **Table 4**. It has been shown that both the particle size and shape have great effects on relative density values.[15,16] D_0 was detected at the point where a measurable force of 100 N appeared. The rank order of D_0 values of different powders was equal, as in tapped densities. The greatest D_0 values, or the most densified powder packing due to the die filling, were observed for batch 2, as the particle and powder properties predicted (**Table 3**). Batch 2 seemed not to have particle rearrangement (D_b) at all, which is hardly true. The most probable explanation for this occurrence is that particle rearrangement already takes place under a force of 100 N and, thus, the part of D_b is virtually larger and D_0 is lower. D_0 values for batches 1 and 3 were the lowest. These values caused the large particle size (eg, large void spaces between spherical particles) observed with batch 1 and unfavorable particle and powder properties, in general, in batch 3. The high D_b values of batches 1 and 3 were caused by the fragmentation of the large particles in batch 1 powder and the disintegration of granules or agglomerates in batch 3 during the rearrange

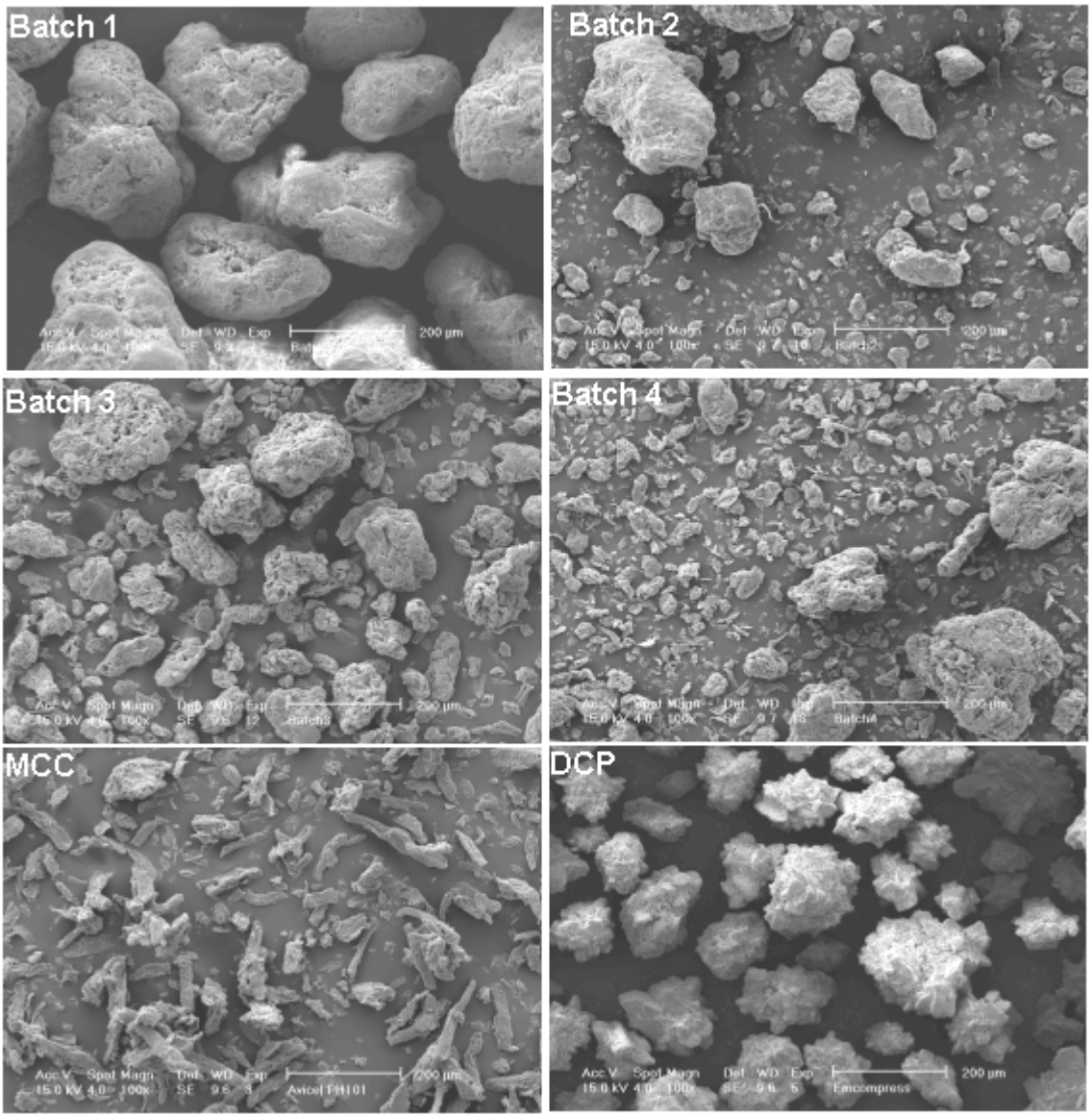

Figure 2. Scanning electron microscope micrographs from powders. Bar is 200 µm. MCC indicates Microcrystalline cellulose; DCP, dicalcium phosphate dihydrate.

ment phase. D_A values of all batches were practically equal. Values of D_b and D_A for starch acetate batches were considerably smaller than those of reference powders. Low D_b values are typically connected to plastically deforming materials.[17,18] Although the particle and powder properties of MCC were predicted to be poor by means of die filling and rearrangement, the small applied force, which took place in D_0 measurement and unexpected large particle rearrangement lead to well-densified powder packing at the beginning of compression.

Compression and tablet properties

The effects of particle properties and water content of the starting material on the volume reduction behavior during compaction and the strength of compacted tablets have been described extensively by several authors.[19-23] In general, a decrease in particle size, an increase in particle surface roughness, and an optimal presence of water in the powder mass will result in stronger tablets, especially with plastically deforming materials. These properties facilitate the volume reduction of powder mass during compaction, resulting in a closer packing of particles in the compact, which leads to a greater bonding surface area to form bonds between particles and, subsequently, to higher compact strength. Mean yield

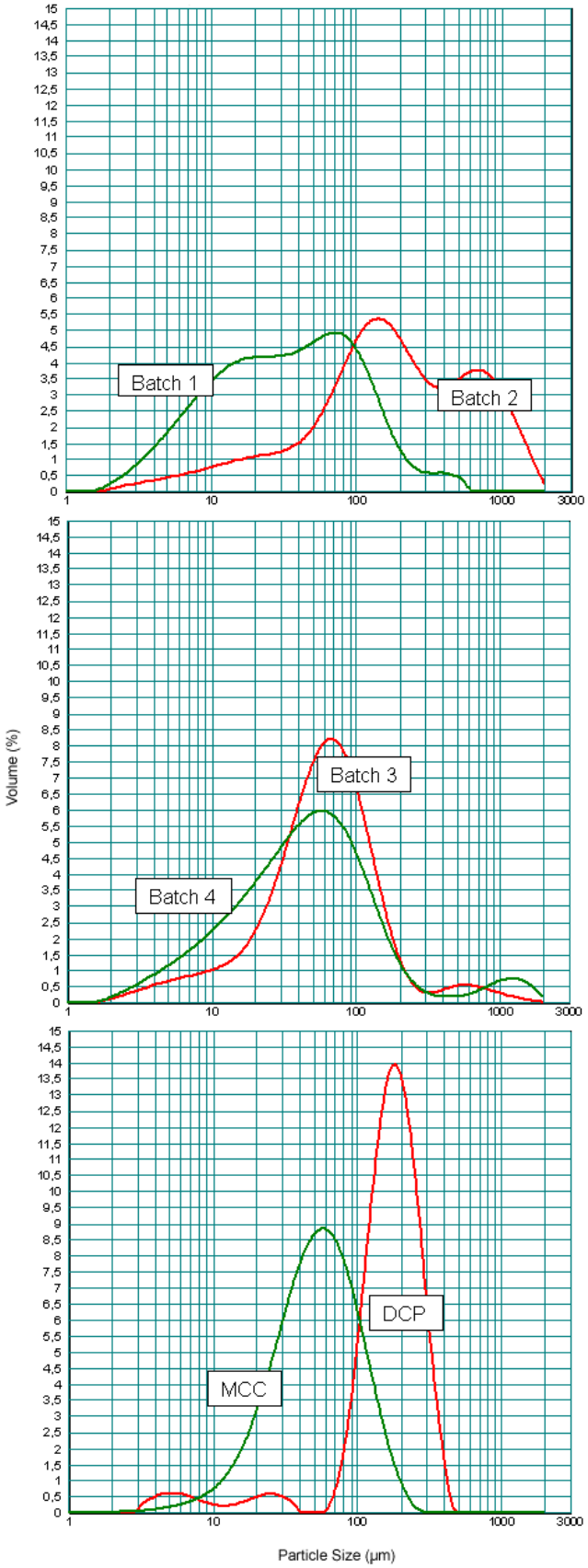

Figure 3. Particle size distributions.

Table 3. Powder Properties*

Drying Method	Bulk Density (g/cm^3)	Tapped Density (g/cm^3)	Angle of Repose (°)	Kawakita Compressibility (a)	Kawakita Cohesiveness (1/b)
Batch 1	0.34 (<0.01)	0.39 (<0.01)	17 (1.5)	0.15 (0.01)	23 (7)
Batch 2	0.44 (<0.01)	0.56 (0.01)	23 (1.3)	0.22 (0.02)	18 (2)
Batch 3	0.32 (<0.01)	0.39 (<0.01)	20 (0.5)	0.19 (0.01)	11 (1)
Batch 4	0.29 (<0.01)	0.40 (0.01)	24 (2.0)	0.28 (0.01)	15 (2)
MCC	0.29 (<0.01)	0.42 (<0.01)	X	0.31 (0.01)	23 (2)
DCP	0.83 (0.01)	0.92 (0.02)	15 (3.6)	0.16 (0.02)	50 (12)

*SD appears in parentheses. MCC indicates microcrystalline cellulose and DCP, dicalcium phosphate dihydrate. X = MCC did not flow through the funnel at all.

Table 4. Compression and Tablet Properties*

Drying Method	D_0	D_b	D_A	P_y (MPa)	Elastic Recovery (%)	Porosity (%)	Tensile Strength (MPa)
Batch 1	0.29 (<0.01)	0.11 (0.01)	0.39 (0.01)	57 (2)	24.5 (0.7)	18.5 (0.3)	9.7 (0.5)
Batch 2	0.41 (<0.01)	0.00 (0.01)	0.41 (0.01)	64 (1)	25.1 (1.2)	20.3 (0.6)	9.5 (0.4)
Batch 3	0.29 (<0.01)	0.13 (0.01)	0.42 (0.01)	66 (1)	20.8 (1.0)	17.4 (0.6)	17.5 (0.5)
Batch 4	0.33 (<0.01)	0.05 (0.01)	0.38 (0.01)	54 (<1)	20.1 (0.6)	14.9 (0.5)	18.1 (0.4)
MCC	0.30 (<0.01)	0.30 (0.01)	0.61 (0.01)	129 (3)	11.1 (0.2)	18.2 (0.2)	15.6 (0.5)
DCP	0.44 (<0.01)	0.28 (<0.01)	0.72 (<0.01)	267 (7)	5.1 (0.5)	18.0 (0.2)	3.6 (<0.1)

*SD appears in parentheses. MCC indicates microcrystalline cellulose and DCP, dicalcium phosphate dihydrate.

pressure (P_y) values of starch acetates varied from 54 to 66 MPa (**Table 4**). Values were approximately half that of MCC, which is known to deform easily by plastic flow. Thus, all starch acetate powders deformed easily under compression, and this result was consistent with the D_b results. Variations in P_y-values of starch acetates were partly due to differing water contents of starch acetate powders (**Tables 2** and **4**). Batch 2 had a high P_y-value and low water content, whereas batches 1 and 4 had the lowest P_y-values and the highest water contents. In the case of batch 3, water content did not correlate with the P_y-value, as it had the highest D_y-value but only moderate water content.

A clear correlation between the particle and tablet properties of starch acetates was observed. Tablets made from batches 3 and 4 were the strongest, having the lowest elastic recovery and low or moderate final tablet porosity. At the same time, these batches also had the smallest particle size, irregular particle shape, greater particle surface roughness, the largest specific surface area, and moderate or high water content. It can be assumed that in the cases of batches 3 and 4, there were numerous contact points and a large bonding surface area to form strong interparticular bonds between the particles, and subsequently firmer tablets. Tablets made of batches 1 and 2 formed weaker tablets. Particle and

powder properties of these powders were unfavorable for interparticular bond formation during compaction. Although the final porosity of the tablets was almost equal between starch acetates and MCC, tablets made of starch acetate powders expanded approximately 2 times more after compression than tablets made of MCC (**Table 4**). However, interparticulate bonds formed in starch acetate tablets were strong enough to allow the stress relaxation without breakage of the tablet (eg, capping) and still, tablets made from batches 3 and 4 were stronger than tablets compressed of MCC.

CONCLUSION

Different functions of dryers induced various water removal processes from the wet material and subsequently affected particle and powder properties. Fluidization of particles in hot air flow (ie, using fluidized bed driers) produced small, irregular, and rough particles having a large specific surface area of moderate powder (bulk density) but excellent tablet properties. Whereas horizontal vacuum rotary driers produced large, spherical, and smooth particles with excellent powder properties but only moderate tablet properties. Overall, these results indicate that some modification of starch acetate can be accomplished by using different driers, but further optimization of the drying processes is still needed.

ACKNOWLEDGEMENTS

The authors are grateful to Ms. Pirjo Hakkarainen for her skillful experimental assistance. The financial support from TEKES (The National Technology Agency of Finland) is gratefully acknowledged. This study was also supported by grants from The Kuopio University Foundation, Eemil Aaltonen Foundation and Pharmacal Research Foundation, Finland.

REFERENCES

1. Korhonen O, Raatikainen P, Harjunen P, Nakari J, Suihko E, Peltonen S, Vidgren M, Paronen P. Starch acetates-multifunctional direct compression excipients. Pharm Res. 2000;17:1138-1143.

2. Raatikainen P, Korhonen O, Paronen P. Particle properties and deformation characteristics of starch acetates. Drug Dev Ind Pharm. 2001;28:165-175.

3. Paronen P, Peltonen S, Urtti A, Nakari J. Starch acetate composition with modifiable properties, method for preparation and usage thereof. US patent 5 667 803. 10/16/1997.

4. York P. Solid-state properties of powders in the formulation and processing of solid dosage forms. Int J Pharm. 1983;14:1-28.

5. York P. Crystal engineering and particle design for the powder compaction process. Drug Dev Ind Pharm. 1992;18(6&7):677-721.

6. Moore JG. Horizontal vacuum rotary dryers. In: Mujumdar AS, ed. Handbook of Industrial Drying. New York, NY: Marcel Dekker Inc; 1987:155-164.

7. Hovmand S. Fluidized bed drying. In: Mujumdar AS, ed. Handbook of Industrial Drying. New York, NY: Marcel Dekker Inc; 1987:165-211.

8. Ludde KH, Kawakita K. Die pulverkompression. Pharmazie. 1966;21:393-403.

9. Heckel RW. Density pressure relationship in powder compaction. Trans Metall Soc AIME. 1961;221(suppl a):671-675.

10. Heckel RW. An analysis of powder compaction phenomena. Trans Metall Soc AIME. 1961;221(suppl b):1001-1008.

11. Fell JT, Newton JM. Determination of tablet strength by the diametral-compression test. J Pharm Sci. 1970;59:688-691.

12. Führer C. Interparticulate attraction mechanisms. In: Aldernborn G, Nyström C, eds. Pharmaceutical Powder Compaction Technology. New York, NY: Marcel Dekker Inc; 1996;71:1-15.

13. Neuman BS, Bean HS, Becket AH, Carless JE. Advances in Pharmaceutical Sciences. 2nd ed. London, England: Academic Press; 1976.

14. Yamashiro M, Yuasa Y, Kawakita K. An experimental study on the relationship between compressibility, fluidity and cohesion of powder solids at small tapping numbers. Powder Tech. 1983;34:225-231.

15. York P. Particle slippage and rearrangement during compression of pharmaceutical powders. J Pharm Pharmacol. 1978;30:6-10.

16. Munoz-Ruiz A, Paronen P. Time-dependent densification behaviour of cyclodextrins. J Pharm Pharmacol. 1996;48:790-797.

17. Doelker E. Recent advances in tableting science. Boll Chim Farm. 1988;127:37-49.

18. Nyström G, Aldernborn G, Duberg M, Karehill PG. Bonding surface area and bonding mechanisms - two important factors for the understanding of powder compactability. Drug Dev Ind Pharm. 1993;19:2143-2196.

19. Ahlneck C, Aldernborn G. Moisture adsorption and tabletting. I. Effect on volume reduction properties and tablet strength for some crystalline materials. Int J Pharm. 1989;54:131-141.

20. Karehill PG, Glazer M, Nyström C. Studies on direct compression of tablets. XXIII. The importance of surface roughness for compactability of some directly compressible materials with different bonding and volume reduction properties. Int J Pharm. 1990;64:35-43.

21. Wong LW, Pilpel N. The effect of particle shape on the mechanical properties of powders. Int J Pharm. 1990;59:145-154.

22. Malamataris S, Karidas T. Effect of particle size and sorbed moisture on the tensile strength of some tableted hydroxypropyl methylcellulose (HPMC) polymers. Int J Pharm. 1994;104:115-123.

23. Nokhodchi A, Rubinstein MH, Ford JL. The effect of particle size and viscosity grade on compaction properties of hydroxymethylcellulose 2208. Int J Pharm. 1995;126:189-197.